

A GRAPHICAL APPROACH TO HEAT AND MASS EXCHANGE BETWEEN GAS AND GRANULAR SOLID

Stanisław Sieniutycz

Faculty of Chemical and Process Engineering,
Warsaw University of Technology,
Waryńskiego Street, No. 1,
00-645 Warszawa, Poland
ssieniutycz@gmail.com

Abstract

A graphical approach to energy and mass exchange in drying-moistening systems is proposed. Advantages of graphical techniques are shown for evaporation-condensation processes in systems with complex gas-solid equilibria, variable gas states, and state dependent properties. Graphical methods are developed for processes with granular solids: drying of single grain, drying in fluidized beds and drying in co- and countercurrent gas-solid flows. Drying time is attributed to each point of a process path in enthalpy chart. Establishment of wet bulb temperature and other asymptotic states are interpreted. Common treatment of graphical solutions and experiments is provided for each drying/moistening period. Unified description of drying operations in all drying periods is achieved.

Key words

Drying modeling, graphical methods, balance and kinetic equations, fluidized beds, countercurrent exchangers, co-current exchangers.

1 Introduction

Processes of evaporation and condensation play an important role in engineering, vapor-generating systems, contact heat exchangers of industrial power equipment, vacuum metallurgy, obtaining of ultra-pure materials and specimens with special properties in microelectronics and different chemical technologies [Chen, 2007]. They also appear in fuel systems of internal combustion engines, cryogenic engines of rockets, and different technological processes of pharmacy industry. From the point of view of exploitation safety, processes of non-stationary evaporation are of special importance in engineering calculations of transient models for vapor-generating systems of powerful electric power plants.

To date, many thermodynamic problems with evapo-

ration and condensation of moisture have extensively been treated; some of the related publications are cited and described in this paper. However, purely analytical or numerical presentation often obscures important thermodynamic properties and hampers their understanding. To improve the situation, [Sieniutycz, 1967], [Ciborowski and Sieniutycz 1969a], and [Ciborowski and Sieniutycz 1969b] attempted to visualize solving methods and solutions to some representative drying problems by using thermodynamic diagrams enthalpy-composition. Suitable graphical representations for experiments follow from the use of graphical methods in thermodynamic charts. The volume limitation of the present paper, which continues and extends these past approaches, does not allow for inclusion of all derivations to make this paper self-contained, thus the reader may need to turn to some previous publications cited here for the purpose.

In the last sixty years [Krischer, 1956], [Luikov, 1966], [Luikov, 1969], [Luikov, 1975], [Luikov and Mikhailov, 1963], [Mujumdar, 2007], [Strumillo and Kudra, 1987], [Kowalski, 2003], [Chen, 2007], and many others, made a significant contribution to scientific basis of the drying theory. In his pioneering books and papers Luikov introduced new integral transformations to solve the system of differential equations of heat and mass transfer in capillary-porous bodies, summarized in his book with Mikhailov [Luikov and Mikhailov, 1963]. Also, [Luikov, 1966] applied disequilibrium thermodynamics and some results of statistical theories to improve the formal theory of evaporating systems. He also obtained a systematic description of heat and mass transfer with a finite propagation. [Mujumdar, 2007] reviewed innovations in industrial drying operations and contributed much to dissemination of novel valuable results in the growing field.

Thermodynamic and kinetic properties (transfer coefficients) are of importance in both analytical and graphical approaches. [Kovac, 1977] applied the theory of

non-equilibrium thermodynamics to multi-component system containing an interface, using a method developed by [Bedeaux et al, 1975]. Evaporation is slow if the resulting velocity field in the vapor is characterized by a low-Reynolds number [Bedeaux and Kjelstrup, 1999]. Kinetic theory predicts a temperature jump across the surface during slow evaporation. Disequilibrium thermodynamics of interfaces similarly predicts a jump. While kinetic theory gives an explicit size of the jump, disequilibrium thermodynamics, without constitutive coefficients, does not. [Bedeaux and Kjelstrup, 1999] expected that disequilibrium thermodynamics reproduces the results found from kinetic theory. The reason for their investigation was to show that kinetic theory together with the boundary conditions is not in conflict with the second law, a fact which has often been questioned. A measurement of the temperature profile, [Fang, 1988] and [Fang and Ward, 1999] has verified the existence of a temperature jump, and found it to be substantial. This measurement proved that the equilibrium condition for the temperature, $T_g = T_l$, like the equilibrium condition for the chemical potential, $\mu_g = \mu_l$, is not fulfilled during slow evaporation. The temperature was found to change almost up to 10K from one side of the surface to another, while the chemical potential was found to change up to about 50J. [Bedeaux and Kjelstrup, 1999] performed an analysis of the experimental results by [Fang and Ward, 1999] who found a temperature jump almost up to 10 K across the evaporating surface of water, octane and methyl-cyclohexane. [Bedeaux and Kjelstrup, 1999] used non-equilibrium thermodynamics to obtain appropriate boundary conditions at the surface. Interfacial transfer coefficients, appearing in these boundary conditions, were determined from the experiments. These authors compared their own results with the predictions for the transfer coefficients stemming from kinetic theory. For three chosen materials the kinetic theory values were found to be 30 to 100 times larger than those found from the experiment. The authors explained why this finding predicts a liquid surface which is colder than the adjacent vapor, contrary to the prediction by the kinetic theory. The relative magnitude that they found for interfacial transfer coefficients, suggests that the condensation coefficient of the kinetic theory decreases with increasing internal degrees of freedom in a molecule. Yet, a lower value of this coefficient is insufficient to explain the small value of the transfer coefficients. As a possible explanation, the researchers forward the hypothesis that the single-particle collision model of the kinetic theory should be modified to account for multi-particle events. These issues still need to be considered in future analytical and graphical approaches.

To exploit full power of thermodynamics methods, classical thermodynamic data of complex gas-solid equilibria must be used together with kinetic equations and data of transfer coefficients. In this paper graphical methods in drying of granular solids are described

and implemented in enthalpy charts for a gas-moisture-solid system. Methods solving kinetic equations in these enthalpy charts are of particular interest. Models of single particle drying, fluidized drying, and drying in countercurrent systems are developed, and their graphical solutions in the enthalpy diagram for gas-moisture-solid are outlined. Drying time is found by integration along process path in the enthalpy chart. Components of drying theory, such as the establishment of wet bulb temperature, are interpreted in the chart. Consistent classifications and representations of graphical solutions and experiments are achieved.

Advantages of graphical methods are explicit for balance-kinetic equations with state dependent coefficients, complex gas-solid equilibria, and variable gas states. Application of these methods is recommended particularly in those cases when developing analytical solution or effective computer program is very difficult or practically impossible to achieve. Both computer programming and graphical methods can help to realize similar goals and overcome similar difficulties. Graphical approaches, however, show clearly and explicitly the interplay between thermodynamic and kinetic properties of considered systems.

The scope of the paper is limited to drying processes with granular solids, for which it analyzes two basic groups of graphical methods:

1. Valuable methods either unpublished or published in local sources not readily available and not in the English language).
2. Newly developed graphical methods to be used in drying practice.

The paper also presents experiments linked with the graphical classification of gaseous and solid paths (graphical solutions). Most of the experiments presented here are original.

The structure of the present paper is as follows. Section 2 focuses on modeling as a common procedure in analytical, numerical and graphical approaches. This section also describes main available papers on current modeling. Section 3 focuses on graphical methods for drying of single grain and batch drying in steady and dynamical fluidized beds. Section 4 develops graphical methods for grain drying in countercurrent, crosscurrent and concurrent gas flows and moving beds. Section 5 imposes a classification of drying paths in enthalpy diagrams, resulting from experiments and from theory. Sec. 6 discusses quantitative properties of typical (non-singular) drying and moistening trajectories in the light of the stability theory (the second method of Liapunov). Section 7 presents briefly concluding remarks. Appendix discusses some related problems and associated articles which treat drying problems by analytical and numerical approaches. All these problems, however, could equally be treated by graphical methods which could provide more effective treatment in the case of state dependent thermodynamic and kinetic coefficients and the case of complex gas-solid equilibria

when obtaining analytical solution or developing effective computer programs is very difficult or practically impossible.

2 Modeling of Moisture Extraction in Drying Systems

A reliable model of practical process of drying or sorption should be sufficiently simple, accurate, and able to capture the process physics and require minimum sets of experiments to generate the unknown parameters. Drying operations satisfy a general scheme of heat driven binary separation process following [Orlov and Berry, 1991].

Chen and coworkers [Chen and Xie, 1997], [Chen and Putranto, 2013] proposed the so-called reaction engineering approach (REA) which has successfully been used to model some drying processes, mainly thin layer drying and drying of small particulates of food materials. Physics of drying is captured by the relative activation energy, which represents the level of difficulty to ‘extract’ moisture of drying in addition to evaporating free water. Initially, the relative activation energy may be zero near the start of drying of high-moisture product and keeps on increasing as the operation progresses. When a low equilibrium moisture content is reached, the relative activation energy becomes one. The relative activation energy of the same materials can be used to model other drying processes with similar initial moisture content. The REA framework offers an effective way of obtaining the necessary parameters. Because of the efficiency of the REA, it is worthwhile to develop it further and to implement it to more complex scenarios. The Reaction Engineering Approach (REA), which captures the basic drying physics, represents an effective mathematical modeling applied to diverse drying processes. The intrinsic “fingerprint” of the drying phenomena can in principle be obtained through a single accurate drying experiment. The book, [Chen and Putranto, 2013], a comprehensive summary of the state-of-the-art and the ideas behind the reaction engineering approach (REA) to drying processes, is a valuable resource for researchers, academics and industry practitioners. Starting with the formulation, modelling and applications of the lumped-REA, it goes on to detail the use of the REA to describe local evaporation and condensation, and its coupling with equations of conservation of heat and mass transfer, called the spatial-REA, to model non-equilibrium multiphase drying. Finally, the volume summarizes other established drying models, discussing their features, limitations and comparisons with the REA. Principles of REA are consistent with CFD modeling applied to various heat and mass transfer processes. These principles are also consistent with general principles of graphical methods, in particular those applied in the present paper.

General equations for simultaneous heat and mass transfer with free enthalpy taken as a universal po-

tential for the moisture transport and the phase transitions have been proposed by [Kowalski, 2003] and [Kowalski and Strumiłło, 1997] who discussed properties of these equations for the boundary conditions characteristic in convective drying of capillary-porous materials. Some applications in the field of drying thermo-mechanics are given in [Kowalski, 2003] and [Kowalski et al., 2000]. In the last paper self-fracturing of fluid-saturated porous materials during drying processes is considered, and a physical model of this widespread phenomenon in drying problems is proposed. The main analysis deals with disperse systems like ceramics, which after drying and calcination become porous bodies with relatively high strength. The emphasis is on two problems: an increase of the cohesive force at the initial stage of drying and de-cohesion of a structure caused by drying-induced stresses.

Some important technological processes in chemical reactors are preceded or followed by drying operations. The use of combustion gases and high-T processes may lead to thermal transformations of previously-dried solids. [Amar et al., 1989] derived the shape of first-stage sinters produced within a framework in which a solid skeleton is wetted by a mobile “liquid” pool. In some cases, significant differences exist between shapes calculated by minimizing the free energy and the assumed shapes. In conclusion the development of effective drying modeling seldom rests on classical thermodynamics, thus the developments based on disequilibrium theories and concepts are necessary.

Investigating conserved property diagrams for rate-process calculations and considering the heat and mass transfer through an interface between two phases, L and G, [Spalding, 1959], [Spalding, 1961] and [Spalding, 1963] presented a derivation of a generalized driving force B , and interpreted the mass transfer coefficient in terms of the Reynolds flux, g . He also recovered the definition of the non-dimensional Stanton number as the ratio g/G .

In the notation used in his book [Spalding, 1963] the mass transfer through the interface satisfies the relationship of the Ohm’s law type,

$$m'' = gB, \quad (1)$$

where the driving force B , following from the conservation law for i -th substance and the transfer property $m_{i,T}$, is obtained in the form

$$B = \frac{m_{i,G} - m_{i,S}}{m_{i,S} - m_{i,T}}. \quad (2)$$

Correspondingly, in Spalding’s model of mass transfer through interface [Spalding, 1963] Reynolds flux g is interpreted in terms of the mass transfer coefficient and the ratio g/G as the non-dimensional Stanton number.

Modelling, analysis and some optimizations of drying systems can be accomplished with the help of thermodynamic diagrams. In their books [Bosniakovic, 1965] and [Ciborowski, 1976] have presented diverse analyses of technical processes on thermodynamic charts. Sugar solutions, which represent a special class of salt solutions, are processed on a large scale in sugar factories. The enthalpy-concentration diagram ($i - x$), which can be used for salt solutions is particularly useful for sugar. The abscissa is chosen to be the water content x , that is the water quantity per unit mass of sugar in the solution. For pure sugar, $x = 0$, for pure water x approaches an infinity. Diagrams $i - x$ for sugar serve to interpret the water vaporization from sugar solutions; similar applications may involve moist coal, sorbents, catalysts, and diverse dried materials, in particular various granular solids in fluidizing systems, [Bosniakovic, 1965], [Ciborowski, 1976], and [Sieniutycz, 1967].

Drying operations are particularly good examples of irreversible processes, associated with appreciable losses. As a consequence, the heat consumption in a drying operation is usually high, thus the task of applied thermodynamics consists of making a drying process closer to its reversible counterpart. In the thermodynamic diagrams, individual irreversibilities can be found and quantified, so that certain understanding of the installation effectiveness is obtained, and a component in which the largest losses occur can be marked for improvement. Analyzes of [Bosniakovic, 1965] involve not only conventional dryers with heat drying agents, but also units removing moisture from the dryer air by the application of work. Diagrams of enthalpy or entropy versus the moisture content serve to show changes of thermodynamic states and to interpret the influence of process components on the overall thermodynamic efficiency of the operation.

3 Graphical Approach to Drying of a Grain and Drying in Fluidized Beds

Figure 1 shows a group of various drying processes between gas and granular solid considered in the present paper. This group involves multistage and continuous countercurrent, co-current and crosscurrent drying of particles falling in dry air or fluidized by dry air, batch fluidized drying, and steady fluidized drying in a horizontal exchanger. Starting with an analysis of a single grain in Sec. 3.1, these processes will be investigated further in the text from the viewpoint of graphical methods.

A large literature currently exists which is related to the drying of single droplets, single granules and granular materials. A relatively new modeling of droplet drying is provided by [Farid, 2003]. He derived a model which predicts the decrease in the droplet mass and temperature when it is immersed in hot air, as in the spray drying of solutions with dissolved solids. He assumes that the droplet experiences first the rapid sen-

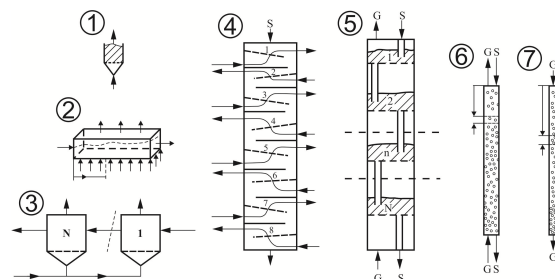


Figure 1. Various drying processes between gas and granular solid: 1 – batch fluidized drying, 2 – steady fluidized drying in a horizontal exchanger, 3,4 – multistage crosscurrent drying, of particles fluidized by air, 5 – multistage countercurrent drying of particles fluidized by air, 6 – continuous countercurrent drying of particles falling in air, 7 – continuous co-current drying of particles falling in air.

sible heating without change of mass, and then the droplet experiences some shrinkage, without temperature change but with the rapid mass decrease. This period is followed by a crust generation period with a remarkable change in the droplet temperature weight, and, finally, a period of nearly-pure heating of the nearly-dry particle. Unlike previous models, Farid’s model takes into account shrinkage and temperature distribution within the droplet. The model also ensures a reasonable estimate for the variation in droplet mass and temperature for a number of experimental measurements available in the literature.

3.1 Drying of Grain by Gas With a State Variable in Time

We begin our studies on graphical approaches with a mathematical description of drying of a single grain in a gas and derivation of an equation which describes the derivative dI/dW in the chart of enthalpy-moisture content for solid phase. For simplicity and brevity of analysis we assume small Biot’s numbers (ignoring distribution of temperature and moisture content within the grain). We also assume the evaporation process on the geometric surface of the grain. In this case equations describing drying dynamics of the grain have the following form:

$$\frac{m_s dI}{F_s dt} = \alpha (t_g - t_s[I, W]) + i_{ps} K'_g (X_g - X_s[I, W]) \quad (3)$$

$$\frac{m_s dW}{F_s dt} = K'_g (X_g - X_s[I, W]) \quad (4)$$

The first describes energy balance and the second mass balance. Square brackets refer to functional relationships which describe the gas-solid equilibrium.

In the problems of simultaneous heat and mass transfer a basic role is played by the overall Lewis factor

$$Le = \frac{C_g K'_g}{\alpha} \quad (5)$$

Assumption of $Le = 1$ which can be made for unbounded water evaporation leads to the simplest equations in which the gas enthalpy differences $i_g - i_s$ appear as the sole driving force for the energy transfer.

$$\frac{m_s dI}{F_s dt} = K'_g C_g (t_g - t_s[I, W]) +$$

$$i_{ps} K'_g (X_g - X_s[I, W]) = K'_g (i_g - i_s[I, W]) \quad (6)$$

For more information see the literature [Sieniutycz, 1967], [Ciborowski and Sieniutycz, 1969a], and [Ciborowski and Sieniutycz, 1969b].

For Le different than one the single driving force in the enthalpy equation can be achieved by using an effective enthalpy defined in terms of enthalpy i_{ts} of a gas with temperature $t=t_g$ and equilibrium humidity X_s . The following formula holds [Sieniutycz, 1967]; [Ciborowski and Sieniutycz, 1969a], [Ciborowski and Sieniutycz, 1969b], [Ciborowski and Sieniutycz, 1969c], and [Ciborowski and Sieniutycz, 1969d].

$$i'_s = i_s Le^{-1} + (1 - Le^{-1}) i_{ts}. \quad (7)$$

In terms of the enthalpy defined above, enthalpy formula (3) takes the form

$$\frac{m_s dI}{F_s dt} = K'_g (i_g - i'_s[I, W]) \quad (8)$$

Division of Eq. (8) by Eq. (4) leads to the slope dI/dW in terms of inlet gas parameters i_g, X_g , and parameters of gas in equilibrium with solid, X_s .

$$\frac{dI}{dW} = \frac{i_g - i'_s[I, W]}{X_g - X_s[I, W]}. \quad (9)$$

The effective equilibrium enthalpy of gas becomes equal to the true equilibrium gas enthalpy is in the case when the Lewis factor Le is equal to one. The simplicity of the slope formula for $Le=1$ follows from mutual

reduction of the effect of heat and mass transfer coefficients. Equation (9) is associated with Fig. 2 which provides a qualitative picture of paths of dried solid grain in the enthalpy-concentration chart for moist solid in the case of drying of a single grain (or a wet bulb) by gas with constant parameters i_g and X_g . In other words Fig. 2 is a graphical representation of Eq. (9) for the constant gas state i_g and X_g . The figure shows that all curves achieve asymptotically the wet bulb temperature or its counterpart attributed to the second drying period. However, the picture is not so simple when the gas parameters i_g and X_g vary along the process path, which occurs, for example, in countercurrent systems. While Eq. (9) still holds, parameters of gaseous and solid phases are linked by balances of mass and energy for finite flows G , and paths depend crucially on the magnitude and sign of the ratio S/G (Sec. 4). The remarkable property of Eq. (9) is its applicability to various drying periods, provided, of course, that the assumptions done while setting Eqs (3) and (4) are satisfied. The formal simplicity of Eq. (9) is not necessary for development of graphical methods but it is convenient for the brevity of analysis.

In fact, simple details of graphical solving of Eq. (9) are not as important as showing that equations of the same structure can be derived for other, more complex, drying processes, such as fluidized drying, packed bed drying, countercurrent drying of falling particles, drying in moving bed systems, etc. Most importantly, Eq. (9) is a valid formula not only for drying of a single grain, but also for a large majority of practical drying systems. In particular, as shown below, Eq. (9) is valid for drying processes in fluidized beds. For operations in which gas parameters change along the process path, such as those in countercurrent and co-current dryers, Eq. (9) is still valid but it must be supplemented by balance equations linking changes of state parameters in gas and solid phases. In all these systems parameters of gas contacting with solid are no longer constant but change along the process path, in a different way dependent on the gas-solid contacting type. In these systems assumption of the constancy of gas parameters must be replaced by a rule of changing of gas state coordinates along the process path, which follows from the enthalpy and mass balances in the gaseous phase.

Figure 2 depicts qualitatively drying paths of a moist solid grain in the enthalpy chart and shows the asymptotic nature of wet-bulb temperature. Qualitatively, this picture may be referred to drying of a single particle or fluidized drying of a solid batch. In the first drying period transient paths of solid fall after a time period into the isotherm of the wet bulb temperature or its counterpart attributed to the second drying period. [Souninen, 1986] discusses effectiveness of psychrometric charts in their application to drying calculations.

Continuous lines in Figure 2 illustrate various paths of solid in the first and the second period of drying. For a sufficiently long time the drying process would

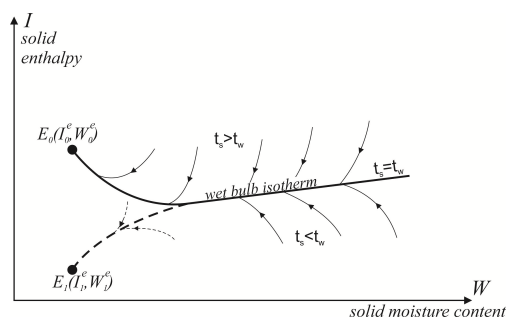


Figure 2. Paths of dried solid grain in the enthalpy-concentration chart for moist solid. All real (continuous) curves achieve asymptotically the wet bulb temperature or its counterpart attributed to the second drying period.

terminate at the point $E_0(I_0^e, W_0^e)$. This point would lie closely to the thermodynamic equilibrium between the final solid and the drying gas. However, the temperature of the solid at this point would be high, thus constituting a hazard to the dried material. In order to avoid high temperatures of the solid, a prescribed distance of the final state of the solid from the equilibrium is required. However, it may be shown that low- T states of the solid, such as, e.g., the one described by the point $E_1(I_1^e, W_1^e)$, cannot be achieved in a single continuous process. Rather a two-stage operation, the first one leading the solid close to $E_0(I_0^e, W_0^e)$ and the second one involving the solid's cooling to $E_1(I_1^e, W_1^e)$ is necessary. The second operation occurs with negligible mass transfer, and may be exemplified by the experimental curve 5 in Fig. 9 in the further text. Summing up, the two-stage control operation solves the problem of sufficiently low temperatures of the final solid, and prevents dangerous exposition of the dried material to high temperatures. See a book, [Sieniutycz and Jeżowski, 2013], for more information about control and optimization problems in grain drying systems.

3.2 Fluidized Drying of Solid by a Gas With a State Variable in Time

We can now pass to drying processes in fluidized beds. While a number of papers appeared to date related to fluidized drying, our interest is focused on those of direct relation to graphical methods. Considering drying models from a single particle to fluidized bed drying, [Tsotsas, 1994] has introduced a normalized single particle drying curve integrated into a generic, heterogeneous fluidized bed model to describe batch fluid bed drying. [Ciborowski and Sieniutycz, 1969c] initiated graphical methods of analysis for basic problems of fluidized heat and mass exchange in thermodynamic diagrams enthalpy-composition. Cases which we shall discuss first as extension of their examples involve the processes of the steady-state fluidized drying with an external heat, shown in Fig. 3 and a batch fluidization in Fig. 4. They involve both balance and kinetic aspects, and they use Eq. (9). The left part of Fig.3 schematizes the steady non-adiabatic opera-

tion, whereas the right one illustrates the two ways of fluidization modeling, first as a pseudo-homogeneous model and the second as a two-phase bubble model. It is the batch fluidization operation for which the application of Eq. (9) will be considered in Fig.4. In further fluidization examples, as those in Figs 5, 6 and 7, kinetic issues can be ignored, and purely thermodynamic approaches are both sufficient and useful.

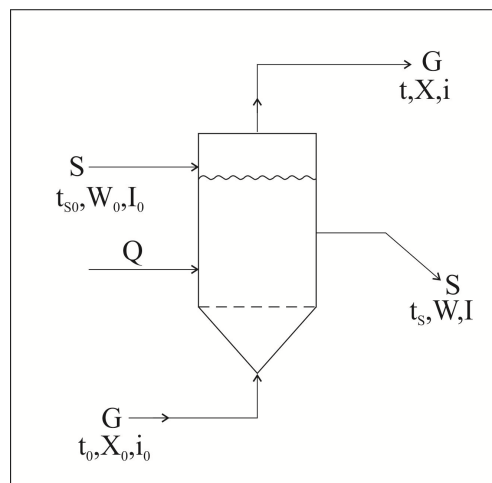


Figure 3. Steady-state operation of non-adiabatic fluidized drying of solid particles. The scheme allows the simultaneous treatment of the batch fluidization and fluidization in a horizontal exchanger.

Chronologically, two ways of modeling of fluidized drying can be distinguished. Case A assumes a model of single mixed pseudo-phase composed of gas and solid particles, [Szwast, 1990], [Sieniutycz, 1991], [Sieniutycz and Jeżowski, 2013]. Case B uses a model composed of a dense, mixed pseudo-phase and a dilute phase with plug flow of bubbles, [Poświata, 2005], [Poświata and Szwast, 2006], as described by [Kunii and Levenspiel, 1991]. All these models allow for a simultaneous treatment of the batch fluidization and fluidization in a horizontal exchanger as a continuous limit of a cascade. Since the models of Kunii-Levenspiel type are quite voluminous and numerous details of their application to fluidized dryers are available in the contemporary literature, [Kunii and Levenspiel, 1991], [Sieniutycz and Jeżowski, 2013], we shall not consider them here. Accepting brevity as a main criterion, we derive dynamical equations for the batch fluidized dryer described by the model of a mixed pseudo-phase, which is sufficient for our purposes here. Yet we extend this model by including a set of equations for a steady operation in a horizontal fluidized exchanger. These equations are derived under the assumption that the gas-solid system in the vertical cross-section of the exchanger constitutes a well-mixed disequilibrium pseudo-phase, [Sieniutycz, 1991], [Sieniutycz and Jeżowski, 2013]. As in the batch fluidization, this is again the case when the outlet gas state i_s

in disequilibrium with solid (I, W). This disequilibrium is associated with a finite value of the number of mass transfer units, N_g .

Assuming an ideal mixing in the fluidizing pseudo-phase of gas and solid, the balances of the energy and mass are described by a set of two equations

$$S_0 \frac{dI}{dt} = G(i_g - i) = K'_g (i - i'_s) \quad (10)$$

$$S_0 \frac{dW}{dt} = G(X_g - X) = K'_g (X - X_s) \quad (11)$$

Index g refers to the inlet gas, whereas the variables without index refer to the unknown state within the dryer. Eliminating parameters of this state from the set of equations (10) and (11) the state equations of a batch fluidization dryer follow in the form

$$\frac{S_0}{G} \frac{dI}{dt} \left(1 + \frac{HTU_g}{h} \right) = i_g - i'_s \quad (12)$$

$$\frac{S_0}{G} \frac{dW}{dt} \left(1 + \frac{HTU_g}{h} \right) = X_g - X_s \quad (13)$$

These are dynamical equations of batch fluidization whose non-dimensional form is represented by Eqs (17) and (18) below.

Modified equations of the form

$$\frac{SdI}{dG} \left(1 + \frac{HTU_g}{h} \right) = i - i'_s \quad (14)$$

$$\frac{SdW}{dG} \left(1 + \frac{HTU_g}{h} \right) = X - X_s \quad (15)$$

describe the drying process in a horizontal fluidizing exchanger, under the assumption of a perfect mixing of both phases in the vertical cross-section perpendicular to solid flow.

We observe that the two considered processes can be described by the same set of equations, provided that the common non-dimensional time τ is defined as follows

$$\tau = Gt/S^0 = G/S \quad (16)$$

where Gt is the cumulative amount of gas supplied after time t to the batch dryer charged by solid amount S^0 , and G/S is the non-dimensional time for the process in the horizontal exchanger. The common set for both processes is

$$\frac{dI}{d\tau} = \frac{N_g (i_g - i'_s(I, W))}{1 + N_g} \quad (17)$$

$$\frac{dW}{d\tau} = \frac{N_g (X_g - X_s(I, W))}{1 + N_g} \quad (18)$$

where $N_g = h/HTU_g$ is the number of mass transfer units. Summing up, our modeling may include the drying process in a horizontal exchanger for which a non-dimensional time τ is simply G/S , where S is constant solid flux and G is the cumulative flux of gas supplied to the horizontal dryer up to achieving the spatial time τ . Since S is constant, the differential $d\tau = dG/S$. We stress that the differential equations (17) and (18) combine both the information contained in the process kinetics and the one contained in the energy and mass balances of two fluidized systems.

With the collaboration of others [Soponnarit et al, 1996] designed, fabricated and tested a cross-flow fluidized bed paddy dryer. This dryer is, in fact, the same unit as the horizontal exchanger considered above. Therefore the approximate model of Eqs. (17) and (18) is applied to the evaluation of the performance of this dryer. [Soponnarit et al, 1997] also studied corn drying in batch fluidized bed dryer. Drying characteristics of corn were investigated. The experimental results indicated that moisture transfer inside a corn kernel was controlled by internal diffusion.

Dividing Eq.(17) by Eq. (18) yields the slope coefficient dI/dW for the considered processes of fluidized drying in the solid enthalpy diagram. The result is again in the form of Eq. (9). Note that, in the case of fluidization, Eq. (9) follows exclusively from balance equations of drying when the thermodynamic equilibrium between the outlet gas and outlet solid can be assumed. For $Le=1$, effective enthalpy coincides with the true equilibrium enthalpy of gas, i.e. $i_g = i_s$. In a more general case of an arbitrary factor Le , effective enthalpy i'_s does in fluidization the same job as in the single particle description. Since Eq. (9) may be applied to variable inlet gas states, it is not unreasonable to surmise that it holds also for countercurrent and concurrent systems. An analysis in Sec. 4 confirms this expectation [Sieniutycz, 1967].

The single pseudo-phase model constitutes an approximate, often insufficient description of fluidization. However it may be used with admissible accuracy (ca. + -12%) in situations where the bed arrangements (baffles, mixers, etc.) cause a significant mixing of fluidized bed, which makes the dispersion contribution to

the plug flow dominant. In the opposite limiting case, that of the negligible dispersion in the gas phase, i.e., when an ideal plug flow of gas can be assumed, the two phase model of fluidization formulated by [Kunii and Levenspiel, 1991]; is operative. Dynamical state equations of this two-phase model are in the most general case implicit.

However, for a majority of real fluidizing apparatuses, where the bed height is of order $0.5m$, practical thermodynamic equilibrium is observed between outlet gas and solid due to the very large specific surface of the solid and very small height of the transfer units (HTU). In this case the number of transfer units N_g , and the limiting state equations (17) and (18), or any other formulas of this sort, are independent of kinetic phenomena, i.e. they describe exclusively equilibrium balances. Needless to say that equilibrium relations in gas-moisture-solid systems may be very complex. Graphical methods often use tables which describe these equilibria in vast range of state parameters [Sieniutycz, 1973].

[Poświata, 2005], and [Poświata and Szwasz, 2006] performed an optimization of drying processes with fine solids in bubbling fluidized beds described by the bubble model of Kunii and Levenspiel. The reader is referred to the book by [Sieniutycz and Jeżowski, 2013], where the bubble two-phase model and results of [Poświata, 2005] and [Poświata and Szwasz, 2006] are described.

[Zahed et al, 1995] modeled numerically the performance of batch and continuous fluidized dryers with diffusion moisture transport in the dense phase particles and interstitial gas-to-particle mass transfer within the dense phase. Their model includes the inter-phase exchange resistance between gas bubbles and the dense phase. It predicts changes of the bed temperature and product moisture content in time. The model is used for both homogeneous and bubbling fluidized bed drying of cereal grains and granular synthetic polymers.

[Ziegler and Richter, 2000] analyzed deep-bed drying in enthalpy-water diagrams for air and grain. With regard to the mean moisture content of the grain, the mass transfer driving forces within the drying zone were computed from the diagram and then related to the measured time course of temperature respectively to the drying rate of the grain. The method led to a thin-layer equation for wheat basing exactly on the thermodynamic relationships between the air and the grain that appear in the drying zone at certain drying conditions. The thin-layer equation was integrated into a mathematical model derived to analyze solar assisted drying of hygroscopic bulk materials and short-time storage of low-temperature heat. The deep-bed drying model was validated for wheat with a good agreement between experimental and simulation results at varied inlet air conditions. [Ziegler and Richter, 2000] proposed an approach in which the enthalpy–water content diagram for moist wheat was combined with the enthalpy–water content diagram for humid air. This is not unlike as

the early graphical approach of [Ciborowski and Sieniutycz, 1969a], [Ciborowski and Sieniutycz, 1969b], [Ciborowski and Sieniutycz, 1969c], and [Ciborowski and Sieniutycz, 1969d]. It can be said that they rediscovered the generalized diagram gas-moisture-solid.

When solid fluxes S in Fig. 3 are reduced to zero but the apparatus still contains a batch of solid particles, drying can be conducted as an unsteady process shown in the right upper part of Fig. 4. This figure outlines basic graphical constructions for the process of batch fluidization in accordance with Eq. (9). Provided that thermodynamic data and enthalpy diagram for the system of gas-moisture-solid are available [Sieniutycz, 1973], [Spalding, 1963]; [Bosniakovic, 1965]; [Ziegler and Richter, 2000], important drying or moistening properties can be derived by graphical constructions which are in principle self-explanatory.

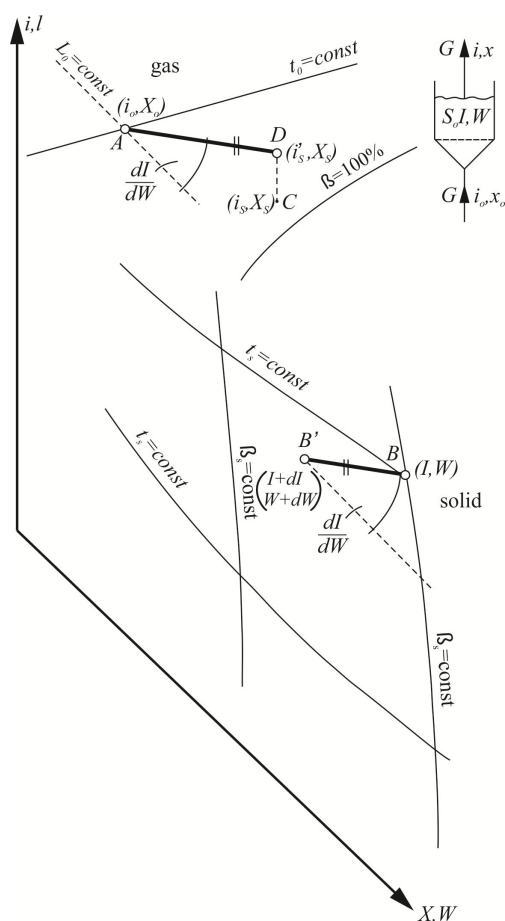


Figure 4. Enthalpy-composition chart for gas-water-solid system. Determining of the local slope dI/dW for the purpose of finding the new solid state in the process of batch fluidization.

The first stage of the multiple use of Eq. (9) is shown in Fig. 4, where the differential slope dI/dW is replaced by its difference counterpart $\Delta I/\Delta W$. Successive iterations lead to a discrete approximation of the solid path $I(W)$ in the enthalpy chart. For a solid state (I, W) located in the solid regime of the enthalpy diagram

the corresponding equilibrium state (i_s, X_s) in the gas regime of the diagram. Next the effective enthalpy is determined from Eq. (7). This allows calculation of the ratio on the right hand side of Eq. (9) which determines the segment B'B with the slope dI/dW . B' is a new state of the moist solid, for which the procedure is repeated. This procedure leads to the solid path $I(W)$ in the solid part of the enthalpy diagram. Summing up, it follows from Eqs (8) and (9) that for the drying of a single granule or a dispersed solid batch dried by a gas with constant parameters, the construction of the solid path in the $I - W$ chart may be performed by sequential determining of local derivatives dI/dW which satisfy the slope equation in the form given by Eq. (9).

We refer the reader to the literature [Ciborowski and Sieniutycz, 1969c] to consider the generalization of the graphical approach in which the balance and kinetic constructions take into account the coefficient of phase changes, ϵ , within the solid phase.

When kinetic effects can be ignored only balance equations are sufficient in graphical constructions. Corresponding examples, of purely thermodynamic nature, are presented in Figs 5-7.

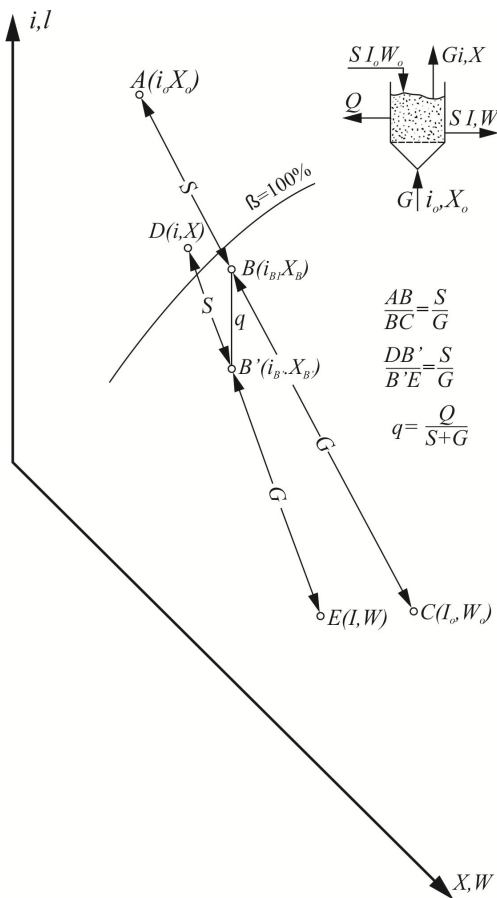


Figure 5. Steady non-adiabatic process of fluidized drying in the enthalpy diagram: effect of heat losses or external cooling.

outlet states of gas and solid in a steady non-adiabatic process of fluidized drying. The example takes into account the effect of heat losses or external cooling. To find outlet states of both phases it is only necessary to realize that the adiabatic mixing of inlet humid gas $G(i_0, X_0)$, point A, with the inlet moist solid $S(I_0, W_0)$, point C, occurs in the enthalpy diagram along the straight line ABC, where point B represents the “adiabatic” two-phase mixture of gas and solid. Since, however, there are usually some heat losses Q , corresponding to unit losses $q=Q/(S+G)^{-1}$, the actual state of the mixture is represented by point B', not B. At point B' gas-solid mixture separates along the two-phase equilibrium straight line DE which leads to the outlet humid gas $D(i, X)$ and outlet moist solid $E(I, W)$.

The moisture content W of outlet solid is lower than the initial W_0 . Clearly, this drying effect can be enhanced in the two-stage or multi-stage process, in which an extra gas flux is directed to the second (next) dryer, to dry the solid leaving the first (previous) dryer. The considered two-stage scheme might be realized in the two-stage cascade shown in the right hand side of Fig. 6. However, the graphical constructions shown in the enthalpy diagram of Fig.6 refer to dryers with external heating rather than to those with external losses of heat. Such dryers ensure lower final moisture contents of solids than the dryer shown in Fig.5.

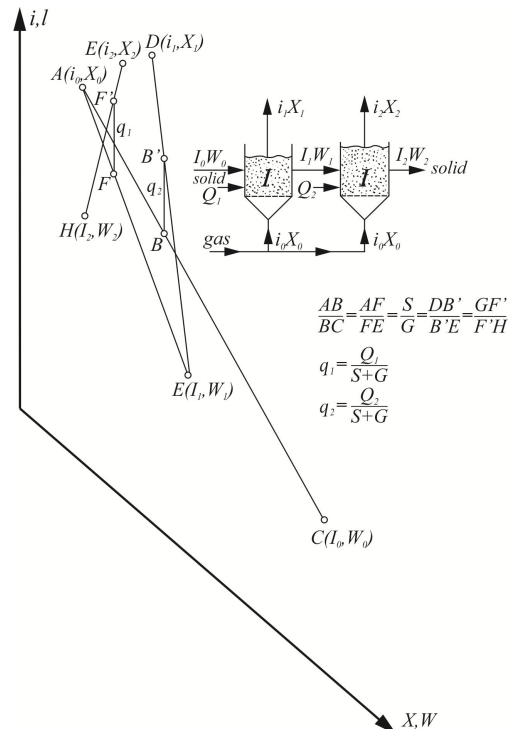


Figure 6. Two-stage, steady fluidized drying with external heating at the stages.

Figure 5 describes constructions aimed at determining

4 Grain Drying in Countercurrent, Crosscurrent and Concurrent Gas Flows

An important family of countercurrent operations of drying and sorption (moistening) includes both continuous and multistage systems. One of these countercurrent operations is depicted in Fig. 7 which describes the case of the multistage fluidized bed with adiabatic sorption. This stage-wise operation involves the dense-phase fluidizations at stages in which outlet gas and outlet solid are in practical equilibrium. As in rectification columns treated by the Ponchon-Savarite graphical method, point B represents the pole of the system, or the state of fictitious mixture that gives rise to the family of operational lines in the form of straight rays launched from point B. Each operational line connects states of gas and solid in the same cross-section of the apparatus. The graphical construction exploits two-phase equilibrium lines, represented in Fig. 7 by straight discontinuous lines - - -. This graphical construction is used to determine the number of theoretical (equilibrium) stages, necessary to achieve a required final concentration of the adsorbed moisture. Dividing this quantity by the mean efficiency leads to the number of real stages when idealized assumption of perfect stages is unacceptable.

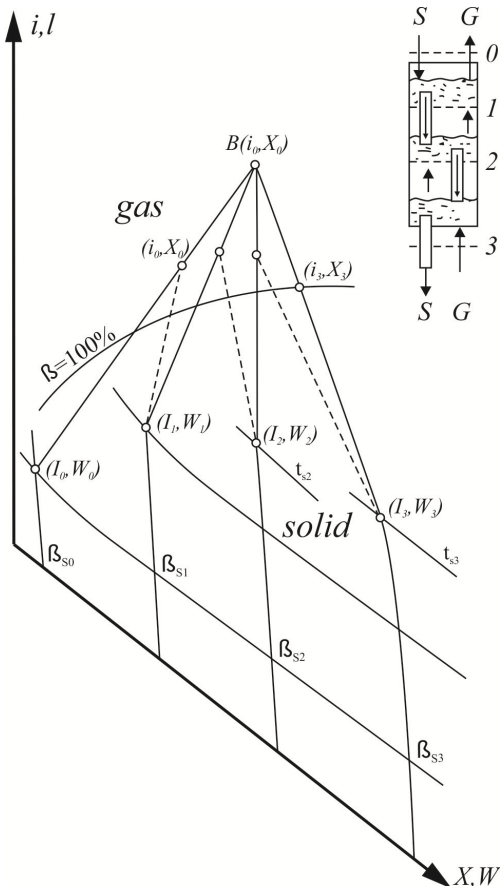


Figure 7. Adiabatic sorption in the countercurrent multistage fluidized bed.

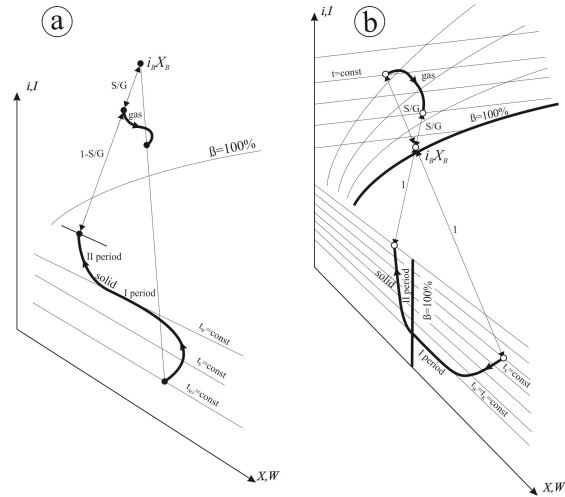


Figure 8. Geometric similarities of gas and solid paths in the enthalpy diagrams for drying in countercurrent system (a) and concurrent system (b).

When kinetic issues are essential, graphical methods for countercurrent (and concurrent) systems include Eq. (9). Since, however, the ratio of solid to gas flows is finite, the method should take into account changes of the gas state in the same cross-section of the dryer. These changes are described by the following differential balances

$$\frac{di}{dI} = \pm \frac{S}{G} \tag{19}$$

$$\frac{dX}{dW} = \pm \frac{S}{G} \tag{20}$$

where the upper sign refers to the countercurrent flow, whereas the lower sign – to the concurrent flow. Equations (9), (19), and (20) constitute a complete set describing continuous concurrent and countercurrent systems. This set determines paths of drying or adsorption processes. By assigning a location coordinate h to path parameters process trajectories can be obtained for all necessary parameters in terms of h . Amongst a number of possible formulas for h in countercurrent and concurrent systems we specify a few below:

$$h = - \int_{T_1}^{T_0} \frac{GC'_g dT}{\alpha a(T - T_s)} = - \int_{X_0}^{X_1} \frac{GdX}{K'_g a(X_s - X)} = - \int_{W_0}^{W_1} \frac{S dW}{K'_g a(X_s - X)} \tag{21}$$

Each integral proves that, in the case of constant coefficients, the length of the dryer is the product of the height of the transfer unit, HTU , and the number of transfer units NTU .

References [Sieniutycz, 1967] and [Ciborowski and Sieniutycz, 1969b] are alternative models. These models assume main transfer resistance in solids and, as such, they use the popular drying coefficient K in place of the overall gas coefficient K'_g used here.

Solid to gas flow ratio, S/G , is one of important factors influencing shapes of gas and solid paths in the enthalpy diagram. The constancy property for the flow ratio S/G along the path in association with energy and mass balances yields the condition of geometric similarity of gas and solid paths in enthalpy diagrams. Figure 8 shows these geometric similarities (left chart for countercurrent system, and right chart for co-current system). Note that in co-current systems the geometric similarity is accompanied with the simultaneous reflection of the gaseous curve.

5 Graphical Classification of Experimental Data

This section links graphical representations with classification of experimental results in enthalpy diagrams. Some limitations of the approach are also discussed.

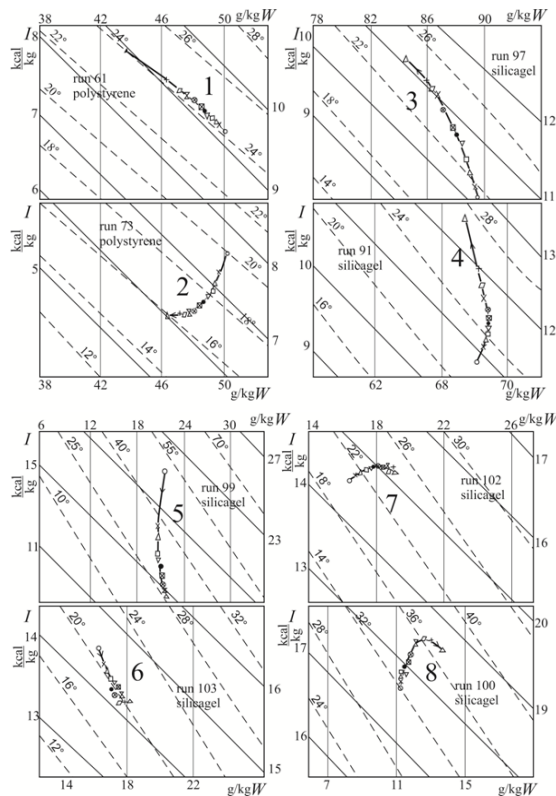


Figure 9. Experimental paths of drying (upper chart) and sorption (lower chart) in the countercurrent flow of gas and granular solid [Sieniutycz, 1967].

Our experiments and study of driving forces in gas

G and solid S in the process of countercurrent drying of falling solid particles show that, qualitatively, in gaseous and solid boundary layers adjacent to the interface, various distributions of driving forces for gas humidity X and solid moisture content W are possible. Some of the distributions may cause appearance of maxima or minima of moisture content, gas humidity, and temperature within each phase, depending on inlet thermodynamic states of solid and gas, total length of the dryer, and values of transfer coefficients. Many of non-typical properties were confirmed by experiments; the results of some of them are shown in Fig. 9.

Figure 9 shows experimental paths of drying (upper chart) and sorption (lower chart) for the countercurrent contact of gas and pulverized solid. Experimental data in Fig. 9 show that there are four typical paths for drying and another four paths for sorption. This limitation is the consequence of constraints imposed by balance equations for gas and solid phases.

Figure 10 shows a basic classification and simultaneous validation of experimental paths of drying and sorption for the countercurrent contact of gas and pulverized solid. This is a “compact classification-validation presentation” for all paths belonging in the same pole. Paths composed of both drying and sorption parts occur. The graph of Fig. 10 describes paths with respect to single saddle point which lies in the origin of the coordinate system (the center point of the graph).

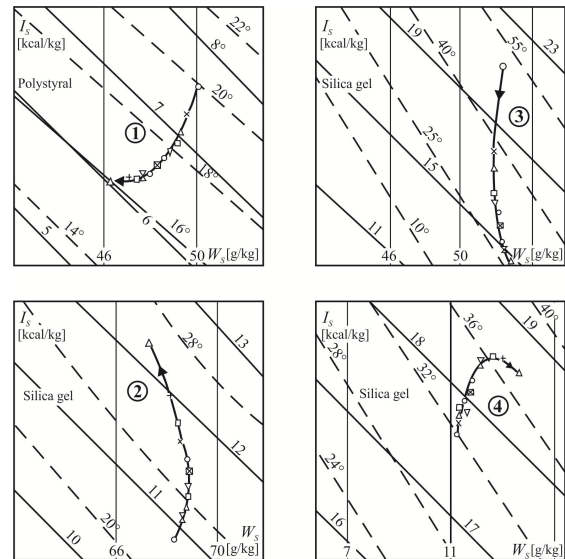


Figure 10. Subclass of paths for the same pole. Experimental paths of drying and sorption located around the singular saddle point in the process of countercurrent contacting of gas and granular solid. The saddle point of trajectories lies in the origin of the coordinate system (the center point of the graph).

Limitations associated with the graphical modeling of drying should not be ignored. In fact, any reasonable graphical approach requires some kind of approximation, such as a single averaged temperature and mois-

ture context of the grain. As confirmed by the counter-current drying experiments [Sieniutycz, 1967], Farid's model, [Farid, 2003], shows that the temperature distribution within the droplet cannot be neglected for a small diameter droplet of $200\mu\text{m}$. This corresponds with the results of some earlier works dealing with granular materials, which state that, not seldom, effects of the temperature distribution within the granules with the inhomogeneous moisture distribution cannot be ignored even for small Biot numbers [Ciborowski and Sieniutycz, 1969b], [Farid, 2003].

Transferring graphical methods to the realm of partial differential equations, [Sieniutycz, 1970] developed principles of graphical approaches to simultaneous heat and mass transfer in packed beds with stationary packing. All constructions were performed on the two-phase diagram for moist gas and moist solid. The method, which involves equations of equilibria, conservation and transfer, holds good for each period of drying or adsorption. It predicts extrema of temperature and absolute moisture content in solid, which move in the direction of the gas flow. Some of predicted properties are not anticipated by oversimplified, isothermal analytic theories of packed beds. The new effects are particularly pronounced in the case of large thermal effects accompanying processes of drying or adsorption.

We refer the reader to the literature for further examples, in particular for balance and kinetic constructions in the gas-water-solid chart which take into account the coefficient of phase changes ϵ within the solid phase [Ciborowski and Sieniutycz, 1969c].

6 Quantitative Properties of Drying-Moistening Paths in The Light of The Stability Theory

This section discusses briefly basic quantitative properties of typical (nonsingular) drying and moistening trajectories in the light of the stability theory (the second method of Liapunov). The results obtained show that the stability conditions for pseudo-equilibrium states in the flow systems (co-current and countercurrent flows) may be determined with the help of quasi-classical potentials (flow potentials), which constitute thermodynamic Liapunov potentials for these systems. For co-current and countercurrent flow systems, a suitable Liapunov function or the difference of Liapunov potentials is the exergy flux of the two-phase gas-solid stream with respect to the exergy flux of this stream at the singular point of zero rates.

$$V = \frac{Gb \pm SB}{G \pm S} - \left(\frac{Gb \pm SB}{G \pm S} \right)_0 \quad (22)$$

where the upper sign refers to the co-current flow, whereas the lower sign – to the countercurrent flow. This criterion can also be expressed in terms of difference between the entropy flux of the two-phase gas-solid stream with respect to the entropy flux of this stream at the singular point of zero rates.

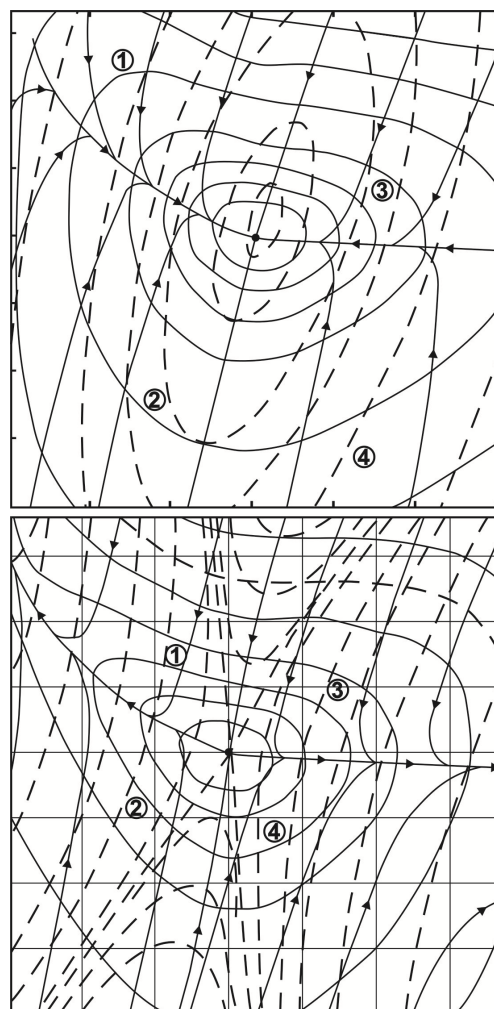


Figure 11. Process paths in the context of Liapunov criteria. Contours of constant Liapunov function \dot{V} (---) and closed continuous contours of constant derivative . Process paths are continuous lines with arrows.

Figure 11 shows a comparison of the cocurrent operation (upper draft) and countercurrent operation (lower draft) between gas and granular solid. In the state space of temperature T (abscissa) and moisture concentration W (ordinate), process paths, i.e. continuous lines with arrows, approach, in the cocurrent case, the singular point of focus type, whereas, in the countercurrent case, they leave the singular point of the saddle type, along two separatrices. Discontinuous contours of constant Liapunov function V (---), represented by the exergy of pole, describe a saddle surface in the countercurrent case and a convex surface with minimum of V in the cocurrent case. Closed continuous contours of constant derivative describe in both cases surfaces of definite sign in accordance with the second law of thermodynamics. Only in the cocurrent case signs of V and dV/dt with respect of process equations are always opposite and, consequently, solid paths approach the stable equilibrium point of focus type. In the countercurrent case, the singular points are saddle type which explains the diverging nature of countercurrent paths.

The methods of stability theory constitute, therefore, an effective tool in prediction of qualitative properties of process paths in gas-solid systems.

7 Concluding Remarks

In the present paper balance and kinetic equations for drying and sorption operations were analyzed and solved in the enthalpy diagram for a gas-moisture-solid system, and principles of thermodynamic classification of qualitative properties of (uncontrolled) trajectories were obtained for various processes of fluidized drying, concurrent and countercurrent drying and adsorption. In this classification four typical trajectories pertaining to drying processes and other four trajectories referred to adsorption are obtained, Fig. 9. Both graphical and experimental data show, under appropriate conditions, extrema (minima or maxima) of temperature and moisture content in the solid phase. All these extrema are predicted by graphical methods and confirmed by the experiments. Graphical methods of analysis in enthalpy-composition diagrams involve the majority of basic problems of heat and mass exchange in fluidized beds.

Importantly, the knowledge and understanding of graphical approaches considerably facilitates transformation of related mathematical models into computer programs. This facility is fortunate in view of the common use of computers at the present time. With recent advancements in mathematical techniques and computer hardware Computational Fluid Dynamics (CFD) has been found to be successful in predicting specific drying phenomena in various types of industrial dryers. As pointed out by [Pakowski and Mujumdar, 2006], we have been witnessing a revolution in methods of engineering calculations. See a review [Jamaledine and Ray, 2010] on application of CFD for simulation of drying processes. Computer tools are now easily available. A new discipline of computer-aided progress design (CAPD) has emerged. Today even simple problems are solved using specialized computer software. General computing tools including Excel, Mathcad, MATLAB, and Mathematica are easily available in any engineering company. Bearing this in mind, [Pakowski and Mujumdar, 2006], have promoted a more computer-oriented calculation methodology and simulation methods to substitute graphical and shortcut methods. Nonetheless they state, "this does not mean that the computer will relieve one from thinking" but that the older methods and rules are still valid "and provide a simple commonsense tool for verifying computer-generated results". In this context one should also see the future role and applicability of graphical methods.

For selection of other drying processes in which the use of graphical methods could be fruitful, book and reviews are recommended [Mujumdar, 1991], [Chua et al., 2002], [Barrozo et al., 2014], [Strumillo and Kudra, 1987]. Appendix below briefly reviews other drying

systems in which graphical approaches can be applied.

8 Appendix: Some Associated Literature Problems

Rates of liquid evaporation based on the statistical rate theory approach and their applications are analyzed by [Fang, 1998]. According to [Fang and Ward, 1999], measurements of the temperature profile across the interface of an evaporating liquid are in strong disagreement with predictions from classical kinetic theory or non-equilibrium thermodynamics. However, the previous measurements in the vapor were made within a minimum of 27 mean free paths of the interface. Since the classical kinetic theory indicates that sharp changes in the temperature can occur near the interface of an evaporating liquid, series of experiments were made to determine whether the disagreement could be resolved by measurements of the temperature closer to the interface. The measurements reported were performed as close as one mean free path of the interface of the evaporating liquid. The results indicate that it is the higher-energy molecules that escape the liquid during evaporation. Their temperature is greater than that in the liquid phase at the interface and, as a result, there is a discontinuity in temperature across the interface that is much larger in magnitude (up to 7.8°C in experiments) and in the opposite direction to that predicted by classical kinetic theory or disequilibrium thermodynamics. The measurements reported therein support the previous data [Fang, 1998].

Mathematical models and numerical techniques for simulation of steady grain drying in countercurrent and concurrent gas flows have been proposed and tested by [Valena and Massarani, 2000]. To overcome numerical difficulties they developed an approach based on simulation starting from initial transient conditions. They also built a laboratory unit to test mathematical models and numerical techniques through the comparison between calculated results and experimental data. However the majority of research in countercurrent and concurrent systems refers to the moving bed dryers. Some of these works are discussed below.

[Jaakko and Saastamoinen, 2005] compared moving bed dryers of solids operating in parallel and counterflow modes. He developed a method used to simulate drying in parallel and counterflow moving beds. He also gave an integral solution showing the relation between time or location in the dryer and degree of drying. The method allows for a rapid calculation of the moisture, vapor mass fraction, and temperature distributions along the dryer in drying with moist air or steam. The method applies to various substances to be dried when the dependence of the drying rate on moisture and ambient temperature and humidity (thin layer drying rate) is known. For the same required degree of drying, unfavorable distribution of the evaporation temperature in the parallel mode increases significantly the size of the cocurrent dryer in comparison to the coun-

terflow dryer. In steam drying, the difference in the size is not so great, since the evaporation occurs approximately at constant temperature.

Theory of moving beds sheds some extra light on modeling of countercurrent systems with falling grains. The aim of work by [Barrozo et al, 1998] was to analyze simultaneous heat and mass transfer between air and soybean seeds in countercurrent and concurrent moving bed dryers by simulation. The equation of drying kinetics was obtained by means of a thin-layer study. The profiles for temperature and humidity of the fluid and the temperature and moisture of the seeds were found by numerical solution of a model consisting of ordinary differential equations. For further work along this line, see papers by Barrozo, Felipe and their coworkers [Felipe and Barrozo, 2003], [Barrozo et al, 2006a], and [Barrozo et al, 2006b]. For a summary on quality of seeds undergoing moving bed drying in countercurrent and crosscurrent flows see especially a review by Barrozo, Mujumdar and Freire, [Barrozo et al, 2014]. The article presents a review of the seed air-drying process, including differential equations models derived from mass and energy balances for seeds and air in fixed and moving bed dryers. The article concludes with an overview of several potential drying technologies that can be applied to seeds.

In the paper by [Djaeni et al, 2008] two-dimensional computational fluid dynamics calculations for multi-stage zeolite drying (adsorbent drying) were performed for two dryer configurations, (1) a continuous moving bed zeolite dryer, and, (2) a discrete bed zeolite dryer. The calculations concern drying of tarragon as a herbal product. The results show the profiles of water, vapor, and temperature in dryer, adsorber, and regenerator. The performance of continuous moving bed zeolite dryer is the best. Residence time of air, product, and zeolite are in accordance to other drying systems. In a latter work of Djaeni group effects of multi-stage adsorption drying are evaluated [Djaeni et al, 2009]. In a multi-stage dryer, the product is dried in succeeding stages while the air leaving a stage is fed to the next stage after dehumidification by an adsorbent. Energy efficiency of the drying system is evaluated for low-temperature drying (10–50°C) and compared with conventional condenser drying. Efficiency of the multi-stage adsorption dryers increases with the number of stages.

[Tórriz et al, 1998] studied theoretically and experimentally drying of grain in a dryer of a crossflow moving bed type. In Sec. 3 a counterpart of this scheme in fluidization is called the horizontal exchanger). The authors analyzed two different dryer configurations, a dryer with central air distribution and another with multiple air ducts. Simulations based on a mathematical model show that distance between inlet air and outlet devices, air to solid flow ratio and dryer height to cross section ratio have a remarkable influence on the process. This conclusion is also valid for countercurrent dryers with falling particles [Ciborowski and Sieni-

tycz, 1969b].

As stated by [Alvarez et al, 2005] product damage, high energy use, and non-homogeneous product properties occur in typical drying operations such as pneumatic drying, fluidized-bed dryers, and upward circulating fluidized-bed dryers. The authors constructed a test for an experimental downflow dryer and modeling of the operation. Predictions of pressure, gas velocity, solid holdup, and temperature agreed with experiments.

[Jaakko and Saastamoinen, 2005] compared the drying rates in moving bed dryers. The gas and the solids to be dried are in parallel flow or counter-flow. Their model is based on the solution of arbitrary experimental or theoretical drying rate Equations of single solid particles (or thin-layer drying rate equation) coupled with heat and mass conservation Equations of the dryer. The solution is presented in an integral form of the drying equation showing the relation between time or location in the dryer and degree of drying. The method allows rapid calculation of the moisture, vapor mass fraction, and temperature distributions along the dryer in drying with moist air or steam. The length of the dryer needed to reach the same degree of drying operating in the parallel mode is much greater than that of counter-flow type.

[Kemp et al, 1994] developed a one-dimensional model and experimental studies of vertical pneumatic conveying dryers. The model takes time increments along the tube; a computer program is required for its implementation. The approach may be used either for initial design or for scale-up from pilot plant data.

[Thakur and Gupta, 2006] examined experimentally drying of high-moisture paddy under stationary and fluidized bed with and without intervening rest periods. Introduction of a rest period between first and second stage of drying improved drying rate and lowered the energy requirement. Fluidization further improved the overall drying process. During the period of rest stage, paddy grain released a considerable amount of moisture as an effect of residual grain temperature. A considerable amount of energy (21–44%) can be saved by providing a rest period from 30 to 120 min between the two stages of drying. Fluidization further reduces (ca 50% against continuous drying under stationary bed) the energy requirement.

[Mujumdar and Law, 2010] discuss trends and applications in postharvest processing in the context of drying technology. Thermal drying technologies have attracted significant R&D efforts owing to the rising demand for improved product quality and reduced operating cost as well as diminished environmental impact. Drying materials may appear in the form of wet solid, liquid, suspension, or paste, which require drying to extend the period of storage, ease of transportation, and for downstream processing to produce value added products. Most of these materials are heat-sensitive and require careful drying; conventional hot air drying can be detrimental to bioactive ingredients. This article

summarizes some of the emerging drying methods and selected recent developments applicable to postharvest processing.

[Nicolin et al, 2014] applied the Stefan problem approach to the mathematical modeling of the diffusion process that occurs during hydration of grains. This technique assumes that the boundaries of the problem are unknown, and finding them is a task, which is part of the problem. The problem has boundaries which move along time. The governing differential equations are numerically solved for the case of transient diffusion, and an analytical solution is obtained for the hydration fronts by considering the pseudo-steady state hypothesis for the diffusion equation. The behavior of hydration fronts is analyzed. The fronts are defined by the moving boundaries and their velocities for both cases. The main differences are analyzed in terms of the transient term of the diffusion equation. The results show the main differences in the behavior of hydration fronts that arise when the transient term is taken into account or the pseudo-steady-state hypothesis is considered and compare the obtained behaviors with experimental data

Currently, energy and exergy analysis are conducted for the purpose of optimizing operating conditions and controlling quality of the products, [Syahrul et al, 2001]. In this context, energy and exergy models are developed for drying of granular materials in fluidized beds, packed beds and other systems with granular solids, in order to evaluate energy and exergy efficiencies. The models and their predictions are subsequently verified against the experimental data. The effects of inlet air temperature, fluidization velocity, slip between phases, and initial moisture content on both energy and exergy efficiencies are studied. Also, the hydrodynamic properties, e.g., the bed holdup, are determined. The results show that exergy efficiencies are lower than energy efficiencies due to irreversibilities which are not taken into consideration in energy analysis, and that both energy and exergy efficiencies decrease with increasing drying time.

It is an open question whether the flux relaxation phenomena of extended irreversible thermodynamics should be taken into account in graphical methods since the effects are usually not substantial. [Mitura, 1981] and [Martynenko and Khramtsov, 2004] analyzed nonstationary evaporation of liquid with the help of the phenomenological thermodynamics of irreversible processes. They stressed importance of evaporation and condensation processes and operations for the contemporary engineering. These processes and operations are present in contact heat exchangers of industrial equipment, vapor-generation systems, vacuum metallurgy, during production of ultra-pure materials and specimens with original properties in microelectronics and diverse chemical technologies. They are also applied in fuel systems of internal combustion engines, rocket cryogenic engines, and in different technological processes of pharmaceutical industry.

From the view point of safety of exploitation, nonstationary evaporation processes are particularly important in engineering calculations of transient models of vapor-generating systems of powerful electric power plants. At present, only the problem of a stationary evaporation–condensation process has been extensively investigated. In fact, analysis of unsteady-state evaporation of liquid served [Martynenko and Khramtsov, 2004] to promote thermodynamics of irreversible processes as the governing, basic theory.

Application of the method of the thermodynamics of irreversible processes in the phenomenological analysis of nonstationary evaporation and the results of experimental study of pressure relaxation in thermostated volume with a sharp change in the vaporization flow indicate the considerable effect of inertial properties of the thermodynamic system in the dynamics of development of a nonstationary process. Thus, in calculation of nonstationary modes of operation of fuel-power equipment we should admit such phenomena as additional vaporization and inductive pressure drop with a sharp change in the vaporization flow. Analytical treatment of these effects is difficult, whereas a graphical approach can work relatively easily.

A subtle topic, associated with three phase systems and graphical methods different than those developed here, is the passage of solids through interfaces, and the system of the differential equations describing a rigid body movement through the boundary of viscous media. A relevant paper in the present journal allows to model various modes of such movement via a singular dynamic optimization problem [Zavalishchin, 2012].

Acknowledgement

This research was supported in 2015 by a grant at Warsaw TU. Fruitful help of Mr Piotr Juszczyk (Faculty of Chemical & Process Engineering, Warsaw TU) in the preparation of graphic part of this paper is gratefully acknowledged.

Nomenclature

a_v	solid surface area per unit volume [m ⁻¹]
B	Spalding's driving force [-]
C_g	specific heat of moist gas per unit mass of dry gas [Jg ⁻¹ K ⁻¹]
c_w	specific heat of moisture in liquid state [Jg ⁻¹ K ⁻¹]
D	diffusion coefficient [m ² s ⁻¹]
F	feed flow rate [kgs ⁻¹]
F_s	solid surface area [m ²]
G	gas mass flux, dry gas base [kgs ⁻¹]
g	Reynolds flux [kgm ⁻² s ⁻¹]
HTU_g	height of transfer unit [m]
h	height of fluidizing layer, distance from inlet [m], unit enthalpy [Jg ⁻¹]
I	solid enthalpy per unit mass of absolute dry solid [kJ kg ⁻¹]
I_0	enthalpy of inlet solid, dry solid base [kJ kg ⁻¹]

I^n solid enthalpy at n-th stage of a cascade [kJ kg⁻¹]
 I_s specific enthalpy of solid phase [kJ kg⁻¹]
 I_0 enthalpy of inlet solid [kJ kg⁻¹]
 i gas enthalpy per unit mass of absolute dry gas [kJ kg⁻¹]
 i_g enthalpy of controlling gas [kJ kg⁻¹]
 i_0 inlet gas enthalpy (dry gas base) [kJ kg⁻¹]
 i_s enthalpy of gas in equilibrium with solid [kJ kg⁻¹]
 i_B enthalpy of pole B , enthalpy of two-phase mixture [kJ kg⁻¹]
 i_c partial enthalpy of moisture in liquid state [kJ kg⁻¹]
 i_p partial enthalpy of moisture in vapor state [kJ kg⁻¹]
 i_{ps} partial enthalpy of vapor in equilibrium with solid [kJ kg⁻¹]
 i_{ts} enthalpy of gas with parameters t and X_s [kJ kg⁻¹]
 i'_s effective enthalpy of gas in equilibrium with solid [kJ kg⁻¹]
 i_0 inlet gas enthalpy [kJ kg⁻¹]
 i_s enthalpy of gas at equilibrium with solid [kJ kg⁻¹]
 K'_g modified overall mass transfer coefficient [kgm⁻²h⁻¹]
 L total length [m]
 $Le = K'_g C_g \alpha^{-1}$ Lewis factor [-]
 l length coordinate [m]
 M_i molar mass of i -th species [kg kmol⁻¹]
 m mass [kg]
 m'' Spalding's mass flux as the product of g and B
 N number of transfer units [-]
 n current stage number [-]
 P thermodynamic pressure [Pa], product flux in Fig.1 [kgs⁻¹]
 Q total heat flux per unit surface area of apparatus [kJm⁻²s⁻¹]
 Q_H, Q_L heat flux density at higher and lower temperature, [kJm⁻²s⁻¹]
 q heat flux density vector [Js⁻¹m⁻²]
 $q = Q(S+G)^{-1}$ heat flux per unit mass of gas-solid mixture [kJm⁻²s⁻¹]
 R universal gas constant [JK⁻¹ mol⁻¹]
 S solid mass flux density, dry solid base [kgm⁻²s⁻¹]
 S_0 dry solid mass in the system [kg or kgm⁻²]
 s specific entropy [J K⁻¹kg⁻¹]
 T temperature of controlled phase [K]
 T_H, T_L higher and lower temperature, respectively [K]
 T_s temperature of solid phase [K]
 t temperature of gaseous phase [oC, K]
 t_s temperature of solid phase [oC]
 t_w wet bulb temperature [oC, K]
 t physical time, contact time [s]
 W water flux in Fig.1 [kgs⁻¹]

W absolute moisture content of solid, dry solid base [gkg⁻¹] [kgkg⁻¹]
 W_e moisture content of solid in equilibrium with gas [gkg⁻¹] [kgkg⁻¹]
 W_0 moisture content of inlet solid [gkg⁻¹] [kgkg⁻¹]
 W_p initial moisture content of solid [gkg⁻¹] [kgkg⁻¹]
 X absolute gas humidity [gkg⁻¹] [kgkg⁻¹]
 X_B humidity of pole [gkg⁻¹] [kgkg⁻¹]
 X_g humidity of controlling gas [kJ kg⁻¹]
 X_0 inlet gas humidity [gkg⁻¹] [kgkg⁻¹]
 X_s humidity of gas in equilibrium with solid [gkg⁻¹] [kgkg⁻¹]
 $\mathbf{x} = (x_1, x_2, \dots, x_i, \dots, x_s, t)$ enlarged state vector of a dynamical process

Greek Symbols

α overall heat transfer coefficient [Jm⁻² s⁻¹ K⁻¹]
 β relative humidity of gas [s⁻¹]
 β_s relative humidity of gas in equilibrium with solid [s⁻¹]
 δ thickness, effective diameter, variation
 ϵ coefficient of phase changes [-]
 μ_k chemical potential of k^{th} component [J kg⁻¹]
 ρ mass density [kg m⁻³]
 ρ_s entropy density [kJ K⁻¹ m⁻³]
 τ non-dimensional time [-]

Subscripts

b bubble
 e energy
 F feed
 g gas
 H high
 k k-th coordinate
 L low, L-surface
 P product
 p interphase
 S S-surface
 s solid bulk
 W water
 v per unit volume
 $1, 2$ first and second phase

Superscripts

e equilibrium
 f final state
 i initial state and time
 n n-th stage number
 T transpose matrix

References

Alvarez, P. I., Vega, R., Blasco, R. (2005). Cocurrent downflow fluidized bed dryer: Experimental equipment and modeling. *Drying Technology* **23**(7), pp.1435–1449.

- Amar, F., Bernholc, J., Berry, R.S., Jellinek, J., Salamon, P. (1989). The shapes of first stage sinters. *J. Appl. Phys.* **65**, pp. 3219–3225.
- Barrozo, M.A.S., Murata, V.V., & Costa, S.M. (1998). The drying of soybean seeds in countercurrent and concurrent moving bed dryers. *Drying Technology* **16**(9-10), pp. 2033–2047.
- Barrozo, M.A.S., Murata, V. V., Assis, A. J. & Freire, J. T. (2006a). Modeling of drying in moving bed, *Drying Technology* **24**(3), pp.269–279.
- Barrozo, M.A.S., Felipe, D. J. M., Sartori, D. J. M., Freire, J. T. (2006b). Quality of soybean seeds undergoing moving bed drying: Countercurrent and cross-current flows. *Drying Technology* **24**(4), pp. 415–422.
- Barrozo, M.A.S., A. Mujumdar, A, Freire, J. T. (2014). Air-drying of seeds: A review. *Drying Technology* **32** (10), pp. 1127–1141.
- Bedeaux, D., Albano, A.M., Mazur, P. (1975). Boundary conditions and non-equilibrium thermodynamics. *Physica A: Statistical Mechanics and its Applications* **82**(3), pp. 438–462.
- Bedeaux, D., and Kjelstrup, S. (1999). Transfer coefficients for evaporation. *Physica A* **270**, pp. 413–426.
- Bosniakovic, F. *Technische Thermodynamik*, I und II. (1965). Dresden: Theodor Steinkopff. See also English edition translated by P.L. Blackshear, Jr.: *Technical Thermodynamics*. (1965). New York : Holt, Reinhart and Winston.
- Chen, X.D. (2007). Simultaneous heat and mass transfer. In *Handbook of Food and Bioprocess Modeling Techniques*. Sablani, S., Rahman, S., Datta, A., Mujumdar, A.S. (Eds). Boca Raton: CRC Press, pp. 179–233.
- Chen, X.D., and Xie, G.Z. (1997). Fingerprints of the drying behavior of particulate or thin layer food materials established using a reaction engineering model. *Trans. I. Chem. Eng. C* **75**, pp. 213–222.
- Chen, X.D., and Putranto, A. (2013). *Modelling Drying Processes: A Reaction Engineering Approach*. Cambridge: University Press.
- Chua, K. J., Chou, S. K., Hawlader, M. N. A., Ho, J. C., & Mujumdar, A. S. (2002). On the study of time-varying temperature drying—Effect on drying kinetics and product quality. *Drying Technology* **20**, pp. 1579–1610.
- Ciborowski, J. (1976). *Basic Chemical Engineering* (Polish). Warszawa: Wydawnictwa NaukowoTechniczne.
- Ciborowski, J., and Sieniutycz, S. (1969a). Fundamental problems of heat and mass exchange in fluidized beds on thermodynamic diagrams enthalpy-composition. (In Polish.) *Chem. Stos.* **6**(2B), pp. 111–125.
- Ciborowski, J., and Sieniutycz, S. (1969b). Graphical methods for investigation of drying of falling particles on thermodynamic diagrams enthalpy-composition. (In Polish.) *Chem. Stos.* **6**(3B), pp. 245–266.
- Ciborowski, J., and Sieniutycz, S. (1969c). Elements de cinetique applique e au sechage a contrecourant de corps finement divises. *Int. J. Heat Mass Transfer* **12**, pp. 479.
- Ciborowski, J., and Sieniutycz, S. (1969d). Untersuchungen der Kinetik der nach dem Gegenstromprinzip durch gefurten Trocknung und Adsorption beim Fallen Zerkleinerter Materialien, *Chemische Techn.* **21**, pp. 750.
- Djaeni, M, Bartels, P. V., Sanders, J. P. M., van Straten, G., van Boxtel, A. J. B. (2008). Computational fluid dynamics for multistage adsorption dryer design. *Drying Technology* **26** (4), pp. 487–502.
- Djaeni, M., van Straten, G., Bartels, P.W., Sanders, J. P. M., van Boxtel, A.J.B. (2009). Energy efficiency of multi-stage adsorption drying for low-temperature drying. *Drying Technology* **27** (4), pp. 555–564.
- Fang, G. *Rate of liquid evaporation: statistical rate theory approach*, Thesis, Graduate Department of Mechanical and Industrial Engineering, University of Toronto, 1998.
- Fang, G., Ward, C.A. (1999). Temperature measured close to the interface of an evaporating liquid. *Phys. Rev. E* **59**, pp. 417.
- Farid, M. (2003). A new approach to modelling of single droplet drying. *Chem. Eng. Sci.* **58**, pp. 2985–2993.
- Felipe, C. A. S., and Barrozo, M. A. S. (2003). Drying of soybean seeds in a concurrent moving bed: Heat and mass transfer and quality analysis. *Drying Technology* **21**(30), pp. 439–456.
- Jaakko, J., and Saastamoinen, J.J. (2005). Comparison of moving bed dryers of solids operating in parallel and counterflow modes, *Drying Technology* **23**(5), pp. 1003–1025.
- Jamaledine. T.J., and Ray, M. B. (2010). Application of Computational Fluid Dynamics for simulation of drying processes: A review. *Drying Technology* **28**(2), pp. 120–154.
- Kemp, I.C., Bahu, R.E., Pasley, H.S. (1994). Model development and experimental studies of vertical pneumatic conveying dryers. *Drying Technology* **12**(6), pp. 1323–1340.
- Kovac, J. (1977). Non-equilibrium thermodynamics of interfacial systems. *Physica A* **86**(1), pp. 1–24.
- Kowalski, S.J. (2003). *Thermomechanics of Drying Processes*. Berlin: Springer.
- Kowalski, S.J., and Strumiłło, Cz. (1997). Moisture transport, thermodynamics, and boundary conditions in porous materials in presence of mechanical stresses. *Chem. Eng. Sci.* **52**(7), pp. 1141–1150.
- Kowalski, S.J., Rajewska, K., Rybicki, A. (2000). Destruction of wet materials by drying. *Chem. Eng. Sci.* **55**, pp. 5755–5762.
- Krischer, O. (1956). *Die Wissenschaftlichen Grundlagen der Trocknungstechnik*. Berlin: Springer.
- Kunii, D., and Levenspiel, O. (1991). *Fluidization Engineering*. Newton: Butterworth-Heinemann.
- Luikov, A. V. (1966). Applications of non-equilibrium thermodynamics to investigations of heat and mass

- transfer. *Intern. J. Heat and Mass Transfer* **9**, pp. 139–152.
- Luikov, A. V. (1969). *Theory of Drying*. New York: Academic Press.
- Luikov, A. V. (1975). System of differential equations of heat and mass transfer in capillary-porous bodies (review). *Intern. J. Heat Mass Transfer* **18**, pp. 1–14.
- Luikov, A.V., and Mikhailov, Y.A. (1963). *Theory of Energy and Mass Transfer* (in Russian). Moscow: Gosenergoizdat. English transl. by L.A. Fenn, (1968), London: Pergamon Press.
- Martynenko, O.G., and Khramtsov, P.P. (2004). Induction relaxation of thermodynamic parameters in non-stationary evaporation. *Int. J. Heat & Mass Transfer* **47**, pp. 2449–2455.
- Mitura, E. (1981). *Relaxation Effects of Heat and Mass Fluxes as a Basis for Classification of Dried Solids*. PhD Thesis. Łódź Technical University, Poland.
- Mujumdar, A. S. (1991). Drying technologies of the future. *Drying Technology* **9**, pp. 325–347.
- Mujumdar, A.S. (2007). An overview of innovation in industrial drying: current status and R&D needs. *Transp. Porous Media* **66**, pp. 3–18.
- Mujumdar, A.S., and Law, Ch. L. (2010). Drying Technology: Trends and applications in postharvest processing. *Food and Bioprocess Technology* **3**(6), pp. 843–852.
- Nicolin, D.J., Jorge, R.M.J., Jorge, L.M.M. (2014). Stefan problem approach applied to the diffusion process in grain hydration. *Transp. Porous Media* **102**, pp. 387–402.
- Orlov, V. N., and Berry R. S. (1991). Estimation of minimal heat consumption for heat-driven separation processes via methods of finite-time thermo-dynamics. *J. Phys. Chem.* **95**(14), pp. 5624–5628.
- Pakowski, Z., and Mujumdar, A.S. (2006). Basic process calculations and simulations in drying. In *Handbook of Industrial Drying*, 3rd edition, pp. 54–79. Mujumdar, A.S.(Ed.), Boca Raton: CRC Press.
- Poświata, A. (2005). *Optimization of Drying Processes with Fine Solid in Bubble Fluidized Bed*. PhD thesis. Faculty of Chemical & Process Engineering, Warsaw Technological University.
- Poświata A., and Szwaśt Z. (2006). Optimization of fine solid drying in bubble fluidized bed. *Transport in Porous Media* **2**, pp. 785–792.
- Sieniutycz, S. (1967). *Investigation of Drying Kinetics when Solid Particles are Falling in a Gas*. PhD Thesis. Warsaw University of Technology.
- Sieniutycz, S. (1970). Simultaneous heat and mass transfer for drying and moistening in packed beds (In Polish). *Chem. Stos.* **7**(3B), pp. 353–368.
- Sieniutycz, S. (1973). Calculating thermodynamic functions in gas-moisture-solid systems. *Reports of Inst. Chem. Eng. Warsaw Tech. Univ.* **2**, pp.71–81.
- Sieniutycz, S. (1991). *Optimization in Process Engineering* (In Polish). 2-nd edn. Warszawa: Wydawnictwa Naukowo Techniczne.
- Sieniutycz, S., Jeżowski, J. (2013). *Energy Optimiza-*
- tion in Process Systems and Fuel Cells*. Oxford UK: Elsevier.
- Soponronnarit, S., Prachayawarakorn, S., Sri-pawaatakul, O. (1996). Development of cross-flow fluidized bed paddy dryer. *Drying Technology* **14**(10), pp. 2397–2410.
- Soponronnarit, S., Pongtornkulpanich, A., Prachayawarakorn, S. (1997). Drying characteristics of corn in fluidized bed dryer. *DryingTechnology* **15**(5), pp. 1603–1615.
- Souninen, M. (1986). A perspective transformed psychrometric chart and its application to drying calculations. *Drying Technology* **4**(2), pp. 295–305.
- Spalding, D. B. (1959). Conserved property diagrams for rate-process calculations. *Chem. Eng. Sci.* **11**: pp. 183–193 and 225–241.
- Spalding, D. B. (1961). Heat and mass transfer between the gaseous and liquid phases of a binary mixture. *Intern. J. Heat Mass Transfer* **4**, pp. 47.
- Spalding, D. B. (1963). *Convective Mass Transfer*. London: Edward Arnold.
- Strumillo, C., and Kudra, T. (1987). *Drying: Principles, Applications and Design*. New York: Gordon and Breach.
- Syahrlul, S. Hamdullahpur, F., Dincer, I. (2001). Exergy analysis of fluidized bed drying of moist particles. *Exergy Int. J.* **0**(0), pp. 1–14.
- Szwaśt, Z. (1990). Exergy optimization in a class of drying systems with granular solids. In *Finite-Time Thermodynamics and Thermoeconomics. Advances in Thermodynamics Series* **4**, pp. 209–248.
- Thakur, A. K., and Gupta, A. K. (2006). Stationary versus fluidized-bed drying of high-moisture paddy with rest period. *Drying Technology* **24**, pp. 1443–1456.
- Tórriz, N., Gustafsson, M., Schreil, A., Martínez, J. (1998). Modeling and simulation of crossflow moving bed grain dryers. *Drying Technology* **16** (9-10), pp. 1999–2015.
- Tsotsas, E. (1994). From single particle to fluid bed drying kinetics. *Drying Technology* **12**(6), pp. 1401–1426.
- Valença, G.C., and Massarani, G. (2000). Grain drying in countercurrent and concurrent gas flow -modelling, simulation and experimental tests. *Drying Technology* **18**(1-2), pp. 447–455.
- Zahed, A.H., Zhu, J.-X. & Grace, J. R. (1995). Modeling and simulation of batch and continuous fluidized bed dryers. *Drying Technology* **13**(1-2), pp. 1-28.
- Zavalishchin, D. (2012). Mathematical model of the motion of a body through a border of multiphase media. *Cybernetics and Physics* **1**(3), pp. 223–226.
- Ziegler, Th., and Richter, L.G. (2000). Analyzing deep-bed drying based on enthalpy-water diagrams for air and grain. *Computers and Electronics in Agriculture* **26**, pp. 105–122.